T-63

UNPUBLISHED PRELIMINARY DATA

32p.

(NASA CR 52237) OTS:

AN APPLICATION OF TIME OPTIMAL CONTROL TO A FLEXIBLE LAUNCH VEHICLE*

J. A. Lovingood +

F. B. Smith, Jr. ++

[1962] refs

N63 23802

CODE-1

23802

Abstract

A minimum response time criterion is used in the design of a pitch attitude controller for a flexible launch vehicle. The criterion is applied to a fourth order model containing the primary dynamics of an assumed thirteenth order vehicle. A collection of time-optimal, open loop trajectories is used to define the closed loop control law. Results of an analog simulation are presented which show that this control law properly applied to the flexible vehicle results in good control.

AUTHOR

*Work reported in this paper was supported by (NASA ~~under~~ contract NASr-27.)

+ Aerospace Engineer, NASA, Marshall Space Flight Center, Huntsville, Alabama (formerly with Minneapolis-Honeywell Regulator Co.)

++ Senior Research Engineer, Minneapolis-Honeywell Regulator Co., MPG Minneapolis, Minnesota

5824008

Introduction

The purpose of this paper is to show that optimal control theory may be applied in the rational design of closed loop regulators for practical plants of high order. The time-optimal criterion applied to pitch attitude control of a flexible launch vehicle serves to illustrate some of the problems involved in applications to significant control problems and to demonstrate some potential solutions. The techniques suggested are of course applicable to a much wider class of problems than the one considered. For example the time-optimal design criterion may be applied to any state variable or any linear combination of the state variables. The truncated model of the complete plant is a suitable model for any design criterion. Similarly, the adjustable logical network used for obtaining and mechanizing the non-linear control law from a collection of open loop trajectories is valuable either for simply mechanizing a known non-linear control law or for obtaining closed loop control according to a control law which is only implicitly defined.

Equations of Motion

The assumed equations of a typical 250,000 pound flexible launch vehicle are given in Table 1. Poles and zeros of the $\frac{\theta_R}{u}$ transfer function are listed in Table 2. Airframe coefficients are taken at the maximum dynamic pressure flight condition with flight speed assumed constant. The equations include dynamics of the rigid body, three body flexure modes, tail-wags dog, actuator, rate servo and an integration of pitch rate for control of pitch attitude. A single control variable is assumed available from gimbaling of the engine.

Specification of the Controller

In applying optimal control theory to the synthesis of controller for practical plants it is necessary to specify both the optimization criterion and what variable or variables are to be controlled. For each criterion such as minimum response time, minimum fuel, minimum error squared, etc., there will be many different choices of controlled variables. Some of these choices will more closely meet the requirements of the physical situation than others. Some of the choices may be completely unacceptable as illustrated by time optimally regulating the state vector of the rigid launch vehicle in Figure 1. When all components of the state vector, pitch attitude, pitch rate, angle of attack and gimbal deflection are brought to zero in minimum time from an initial displacement in pitch attitude of 0.01 radian, displacements of attitude and angle of attack greater than 0.15 radian occur. Although this is the time-optimal response for regulation of the state vector, it is certainly not acceptable since it would literally destroy the vehicle. On the other hand, if the problem posed is that of bringing the single component, pitch attitude, to zero in minimum time and holding it there then the deadbeat response to step input of attitude is obtained (Figure 1). In this case angle of attack and gimbal deflection are not zero at the response time (time when θ and $\dot{\theta}$ are first zero) but decay with a 21.7 second time constant characteristic of the plant. Single component control such as this can be described as motion to a region in the n-dimensional space. The target region is determined as that region in n-space where the component being controlled is zero and is capable of being held there with a bounded control variable. (Reference 1, 2). The necessary and sufficient conditions for minimum time motion to such a region have been obtained (Reference 3).

In the work presented in this paper, optimum control synthesis techniques are demonstrated for control of pitch attitude. The controller obtained is fourth order, one dimensional. That is, the control variable is a function of four variables, and the target set is a line segment in this four-space. Choice of pitch attitude was arbitrary. The techniques apply equally as well to control of other components of the state vector or to control of a linear combination of them such as minimum drift.

A Truncated Model

Although time-optimal control theory applies in principle to regulation of plants of any order, it is not desirable nor necessary to apply it in controller design to the complete plant representation when the motion of the variable being controlled is primarily influenced by relatively few variables. In the launch vehicle considered, the flexure mode frequencies are quite high and aero-dynamic coupling small so flexure has only minor effects on rigid body pitching motion. The same is true of the actuator dynamics. Consequently there is a natural division of the plant into a set of dominant and a set of secondary dynamics. Time-optimal synthesis is applied to control the dominant modes only, and conceptually the secondary dynamics act as a filter on the primary modes. This is shown in Figure 2. The transfer function $\frac{\theta_R}{u}$, for the entire plant of Table 1, has been divided into two parts

$$\frac{\theta_R(s)}{u(s)} = G_1(s) \cdot G_2(s) \qquad (1)$$

Primary dynamics are contained in

$$G_1 = \frac{0.8808\ (s + 0.0478)}{s(s+0.02)(s - 1.4296)(s+1.4964)} \qquad (2)$$

and secondary dynamics in G_2. Feedback of the fictitious output of G_1 is used for controller design. The partial principle coordinate methods of Reference 4 permit one to derive the linear transformation relating the y coordinates to the state of the system, x. The transformation

$$y = Lx \tag{3}$$

where y is an m-vector, L an mxn-matrix and x an n-vector, in general, then permits the fictitious control loop of Figure 2 to be changed to the one which is physically realizable in Figure 3.

A plant in state vector form which gives the transfer function of equation (2) is,

$$\begin{bmatrix} \dot{y}_1 \\ \dot{y}_2 \\ \dot{y}_3 \\ \dot{y}_4 \end{bmatrix} = \begin{bmatrix} 0 & 1 & 0 & 0 \\ 0 & -0.0394 & 2.1403 & -4.404 \\ 0 & 1.00 & -0.02738 & -0.04213 \\ 0 & 0 & 0 & -0.02 \end{bmatrix} \begin{bmatrix} y_1 \\ y_2 \\ y_3 \\ y_4 \end{bmatrix} + \begin{bmatrix} 0 \\ 0 \\ 0 \\ 0.2 \end{bmatrix} u \tag{4}$$

This was obtained by deriving $\frac{y_1(s)}{u(s)}$ and $\frac{y_3(s)}{u(s)}$ transfer functions from a set of equations of this form but with unknown coefficients and then adjusting coefficients to give the proper poles, zeros and gains. A similar set of equations could be obtained directly from the transfer functions of equation (2) and the transformation to continuous coordinates of Reference 5.

The transformation matrix L, which relates the output of the flexible vehicle to the y variables contains many elements which are very small. It is possible to neglect these. The transformation used in the analog simulation was,

$$\begin{bmatrix} \theta_F \\ \dot{\theta}_F \\ \alpha_F \\ \delta_F \end{bmatrix} = \begin{bmatrix} y_1 \\ y_2 \\ y_3 \\ y_4 \end{bmatrix} = \begin{bmatrix} 1 & 0.0341 & 0 & 0 & 0 \\ 0 & 0.999 & 0.0729 & 0 & 0.15 \\ 0 & 0.0341 & 0.999 & 0 & 0.0016 \\ 0 & 0 & 0 & 1 & 0 \end{bmatrix} \begin{bmatrix} \theta_R \\ \dot{\theta}_R \\ \alpha_R \\ \delta_c \\ \delta_e \end{bmatrix} \tag{5}$$

Because of the close correspondence of the y's with the rigid body variables, a new set of variables $\theta_F, \dot{\theta}_F, \alpha_F, \delta_F$, is defined in equation (5). Motion of θ_F corresponds very closely with that of θ_R, so it is reasonable to take equation (4) as the truncated model of the full system.

Two points should be emphasized in the choosing of a truncated model for controller design. First, division of the plant into primary and secondary dynamics cannot be made until the variable to be controlled has been specified. This variable may be one of the physical variables appearing in the state vector x or may be a linear combination of them. Second, even if the secondary dynamics are a result of a limited number of physical variables in the equations of motion, (Table I), the primary dynamics cannot be obtained by simply neglecting these variables and equations. For example, if the equations for the flexure modes and actuator were omitted in truncating to a fourth order model corresponding to G_1, the poles at -1.4962 and 1.4296 would be at -1.47 and 1.403.

Closed-Loop Time-Optimal Control Law

The next step in the synthesis procedure is to derive a closed-loop controller for the model of equation (4). The criterion for design is time-optimal regulation of pitch attitude; that is θ_F is to be brought to zero from an initial condition in minimum time subject to a bounded control variable, and then held at zero. This corresponds to motion to a one dimensional line segment in the four dimensional space of θ_F, $\dot{\theta}_F$, α_F, θ_F.

There is no known method for obtaining a useful closed form expression for the closed-loop control law u(x) which moves the plant to the desired line segment optimally. However, it is possible to compute open-loop solutions u(t,x(0)) for any initial condition x(0) using the computational techniques described in Reference 6. These techniques solve a set of transcendental equations for a control variable u(t,x(0)) which is constrained to satisfy the maximum principle. Since the maximum principle has been shown to be a necessary and sufficient condition for the optimum solution, the u(t,x(0)) obtained is the optimal one. It is not practical to solve the required equations on line to achieve effective closed-loop control. Instead a collection of open-loop optimum trajectories from a set of initial conditions distributed evenly throughout the phase space region of interest is used to define a closed-loop control law by the method described in Reference 7. Each of the variables θ_F, $\dot{\theta}_F$, α_F, and δ_F is divided up into 32 regions called quanta. A Boolean variable X_i^j, is defined for each quantum ($i = 1, 2, 3, 4$, $j = 1, 2, \ldots 32$). The variable X_i^j takes a value one if the measured magnitude of the i^{th} variable is within the j^{th} region and takes the value zero if the magnitude is within any other region. A logic form,

$$u(x) = \text{sign}\left[\sum_{i=1}^{4} \sum_{j=1}^{32} X_i^j \lambda_i^j\right] \qquad (6)$$

is assumed capable of mechanizing the control law and the 128 constants, λ_i^j, are experimentally adjusted to make $u(x)$ agree with the optimum control variable discrete points on the optimum trajectory. This adjustment or training procedure is shown in Figure 4. Switch S is opened at $t = 0$ and the open-loop optimal solution $u(t)$ applied to the simulated plant. Output of the plant $x(t)$, is the input to the logical net and the output of the net $u(x(t))$, is compared with the optimum control variable $u(t, x(0))$ at discrete intervals of time. If the control variables are different, the λ_i^j corresponding to the X_i^j's which are one for that $x(t)$ are incremented in the direction to make the sign of their sum the same as the sign of $u(t,x(0))$. If $u(x(t))$ and $u(t,x(0))$ are the same then no adjustment is made. This procedure was carried out on a general purpose digital computer using a set of 198 optimum trajectories for the plant of equation (4), distributed in the space,

$$\begin{array}{rcccl} 0 & \leq & \theta_F & \leq & 0.1 \\ -0.12 & \leq & \dot{\theta}_F & \leq & 0.12 \\ -0.1 & \leq & \alpha_F & \leq & 0.1 \\ -0.12 & \leq & \delta_F & \leq & 0.12 \end{array} \qquad (7)$$

Control variable comparison points were at intervals of 0.1 second. As the adjustment is carried out, the number of differences (called errors) between $u(x(t))$ and $u(t,x(0))$ is an indication of the convergence of the procedure. The per cent errors, $100\,\frac{\text{No. of errors in N points}}{N}$, is plotted as a function of the number of trajectories in Figure 5. First switch points are those between $t = 0$ and the first switch time, second switch points between the first switch time and the second, etc. Initial λ_i^j were all taken to be zero. It is seen that errors drop very rapidly at first, being less than 10 per cent after only 100 trajectories. At 5000 and 7500 trajectories the resolution of the logic of equation (6) is artificially increased by multiplying all λ_i^j's by two. At 11,000 trajectories the λ_i^j's are multiplied by a factor of ten. Typical closed-loop control responses using the logic at the stages of training shown in Figure 5 are presented in Figure 6. At 198 trajectories the controller has not yet stabilized the statically unstable vehicle. At 2100 trajectories the closed loop is apparently stable but responses are poor. At 11,000 trajectories responses closely approximate optimum. (Limited hardware did not permit evaluation of closed-loop responses at 13,500 trajectories). The logic of equation (6) with constants at 11,000 trajectories is taken as the closed-loop controller for the plant of Table 1.

The slow convergence of the training procedure shown in Figure 5 should not be taken as typical. In the case shown, the initial constants λ_i^j were taken equal to zero and after repeating the 198 trajectories three times, the rate of reduction in errors was limited primarily by build-up of the magnitudes of the λ_i^j's. Convergence to a good controller can be speeded up by several means including starting with λ's corresponding to a planar approximation to the surface, or by multiplying the λ's by a constant at 600 trajectories instead of at 5000. Even without these speed-up procedures however, the computer time to obtain the final controller used was not prohibitive. Approximately five hours of Honeywell-800 computer time were used to obtain 500 optimum solutions, compute trajectories for 198 of these and store them on tape and then adjust the logic as described in the text and shown in Figure 5.

Control of the Flexible Vehicle

A block diagram of the control system is given in Figure 7. Mechanization of the logical net for this optimal control of the fourth order plant was accomplished using standard, commercial analog to digital converters for quantization and diode-transistor logic in conjunction with standard ladder networks to form the logic of equation (6) (Reference 7). A linear switching mode of the control variable was used when the plant output was within approximately one quantum of the target set. This reduced residual errors due to switching on a quantized switching surface and held the plant within the target set. The linear switching used in this mode was,

$$U = \text{sign}\left[\theta_F + 1.25\,\dot{\theta}_F + 0.65\,\ddot{\theta}_F\right]$$

No attempt was made to minimize the steady state limit cycle with the control variable in this mode.

Two schemes for measurement of the variables fed back to the controller were investigated. The first measured the state of the system using the method of Reference 8 which uses a complement of n sensors in measuring the state of an n^{th} order system. In the second, a rigid body pitch rate signal was derived using the phase blending technique of Reference 9. This provided a signal which could be freed of first mode influence, however in this case a slight amount of first mode feedback was included in the signal to damp the first mode bending.

Typical analog responses are shown in Figures 8, 9, 10, and 11. Rigid body pitch attitude responses are quite similar for rigid body feedback and for blender feedback of pitch rate. The small amount of first mode feedback (blender gain $K_1 = 0.9$) causes the first mode to damp out with the blender system whereas with rigid body feedback there is a sustained oscillation. When the blender gain K_1 was set to cancel all first mode feedback ($K_1 = 1.0$), the blender system also exhibited a sustained oscillation of the first mode. Responses to 40-fps sharp-edged gusts are shown in Figure 10. The single component attitude regulator essentially ignores the gust disturbance and maintains the desired attitude. Figure 11 illustrates response to various command inputs. Although the system was designed to approximate time optimal regulation, it exhibits a very good following capability.

Conclusion

It has been shown that the collection of experimental procedures and theoretical knowledge is sufficient to use a time-optimal regulation criterion for rational design of controllers for a high order plant with known coefficients. The synthesis procedure includes obtaining a representative set of open-loop optimum trajectories for a truncated model which is based on the dominant dynamics of the plant. The set of open-loop trajectories is used to define a closed-loop control law for the model. When this controller is applied to the full plant, the output is effectively that of the optimally controlled model filtered by the secondary dynamics of the plant. The resulting controller is relatively simple. However measurement requirements are severe in that the entire state of the system must be measured. This is feasible using the methods of Reference 8 but undesirable because of the large number of sensors required. Such schemes as the gyro blender give promise of relaxing these requirements.

References

1. Lee, E. B., "On the time-optimal regulation of plants with numerator dynamics", IRE Transactions on Automatic Control, Vol AC-6 No. 3, p. 351, September 1961.

2. Harvey, C. A., "On determining the switching criterion for time-optimal control", International Symposium on Nonlinear Differential Equations and Nonlinear Mechanics, Colorado Springs, Colorado, July 1961.

3. Harvey, C. A. and Lee, E. B., "On the uniqueness of time-optimal control for linear processes", Journal of Mathematical Analysis and Application, 1962.

4. Lovingood, J. A., "Approximations to state vector control", Adaptive State Vector Control, MH-MPG Report 1529-TR7, 31 May 1962 (Available from NASA).

5. Laning, J. H. and Battin, R. H., RANDOM PROCESSES IN AUTOMATIC CONTROL, McGraw-Hill Book Co., Inc., New York, 1956.

6. Stone, C. R., Smith F. B., and Lovingood, J. A. "An introduction to self-evaluating state vector control of linear systems", Adaptive State Vector Control, MH-MPG Report 1529-TR1, 13 June 1962 (Available from NASA).

7. Smith, F. B., "A logical net mechanization for time-optimal regulation", Adaptive State Vector Control, MH-MPG Report 1529-TR8, 15 August 1962 (Available from NASA).

8. Harvey, C. A., "Measurement of the state vector", Adaptive State Vector Control, MH-MPG Report 1529-TR3, 15 March 1962 (To be published as a NASA tech note).

9. Lee, R. C. K. and Falkner, V. L. "Adaptive control systems for large elastic boosters", 1960 IRE Symposium on Adaptive Control Systems, Garden City, Long Island, October 17-19, 1960.

Table 1. Critical frequencies of $G(s) = \frac{\dot{\theta}_R(s)}{U(s)}$

Static gain of airframe = 0.0985 rad/rad

Source	Poles	Zeros
Pseudo - Integrator	-0.02	--
Actuator	-30 $-6.5 \pm j\,65\sqrt{0.99}$	--
Rigid Body	1.4296 -1.4964	-0.0478
Tail Wags Dog	--	$-0.0233 \pm j\,57.00$
First Bending Mode	$-0.0962 \pm j\,18.00$	$-0.120 \pm j\,17.77$
Second Bending Mode	$-0.233 \pm j\,46.34$	$-0.225 \pm j\,46.81$
Third Bending Mode	$-0.479 \pm j\,92.69$	$-0.454 \pm j\,94.35$

Table 1. Equations of Plant in Standard Form

$$
\begin{bmatrix} \dot{\theta} \\ \ddot{\theta} \\ \dot{\alpha} \\ \dot{\delta}_c \\ \dot{\delta}_e \\ \ddot{\delta}_e \\ \dddot{\delta}_e \\ \dot{\xi}_1 \\ \ddot{\xi}_1 \\ \dot{\xi}_2 \\ \ddot{\xi}_2 \\ \dot{\xi}_3 \\ \ddot{\xi}_3 \end{bmatrix}
=
\begin{bmatrix}
0 & 1 & 0 & 0 & 0 & 0 & 0 & 0 & 0 & 0 & 0 & 0 \\
-0.04119 & 2.044 & 0 & -4.296 & 0 & -0.00132 & -0.007378 & -0.4351(10^{-4}) & 0.07056 & 0.9747(10^{-5}) & -0.14405 & 0.1619(10^{-4}) \\
-1.00003 & -0.02484 & 0 & -0.044529 & 0 & -0.00001234 & -0.11798(10^{-3}) & -0.49797(10^{-6}) & +0.4372(10^{-3}) & 0.22946(10^{-6}) & -0.00155 & -0.56710(10^{-6}) \\
0 & 0 & -0.02 & 0 & 0 & 0 & 0 & 0 & 0 & 0 & 0 & 0 \\
0 & 0 & 0 & 0 & 1 & 0 & 0 & 0 & 0 & 0 & 0 & 0 \\
0 & 0 & 0 & 0 & 0 & 1 & 0 & 0 & 0 & 0 & 0 & 0 \\
0 & 0 & 128000 & -128000 & -4360 & -43.6 & 0 & 0 & 0 & 0 & 0 & 0 \\
0 & 0 & 0 & 0 & 0 & 0 & 0 & 1 & 0 & 0 & 0 & 0 \\
16.5905 & 1036.0 & 0 & 4794.7 & 0 & 1.6409 & -322.8 & -0.19485 & -65.777 & -0.022106 & 185.61 & 0.037698 \\
0 & 0 & 0 & 0 & 0 & 0 & 0 & 0 & 0 & 1 & 0 & 0 \\
-1.52804 & 231.44 & 0 & -4448.5 & 0 & -1.6509 & -2.9269 & -0.014518 & -2151 & -0.46564 & -177.74 & -0.025685 \\
0 & 0 & 0 & 0 & 0 & 0 & 0 & 0 & 0 & 0 & 0 & 1 \\
75.0402 & -3744.6 & 0 & 5214.5 & 0 & 2.409 & -8.3915 & +0.07525 & -118.32 & -0.013664 & -8589.2 & -0.95553
\end{bmatrix}
\begin{bmatrix} \theta \\ \dot{\theta} \\ \alpha \\ \delta_c \\ \delta_e \\ \dot{\delta}_e \\ \ddot{\delta}_e \\ \xi_1 \\ \dot{\xi}_1 \\ \xi_2 \\ \dot{\xi}_2 \\ \xi_3 \\ \dot{\xi}_3 \end{bmatrix}
+
\begin{bmatrix} 0 \\ 0 \\ 0 \\ +0.2 \\ 0 \\ 0 \\ 0 \\ 0 \\ 0 \\ 0 \\ 0 \\ \\ 0 \end{bmatrix} u
$$

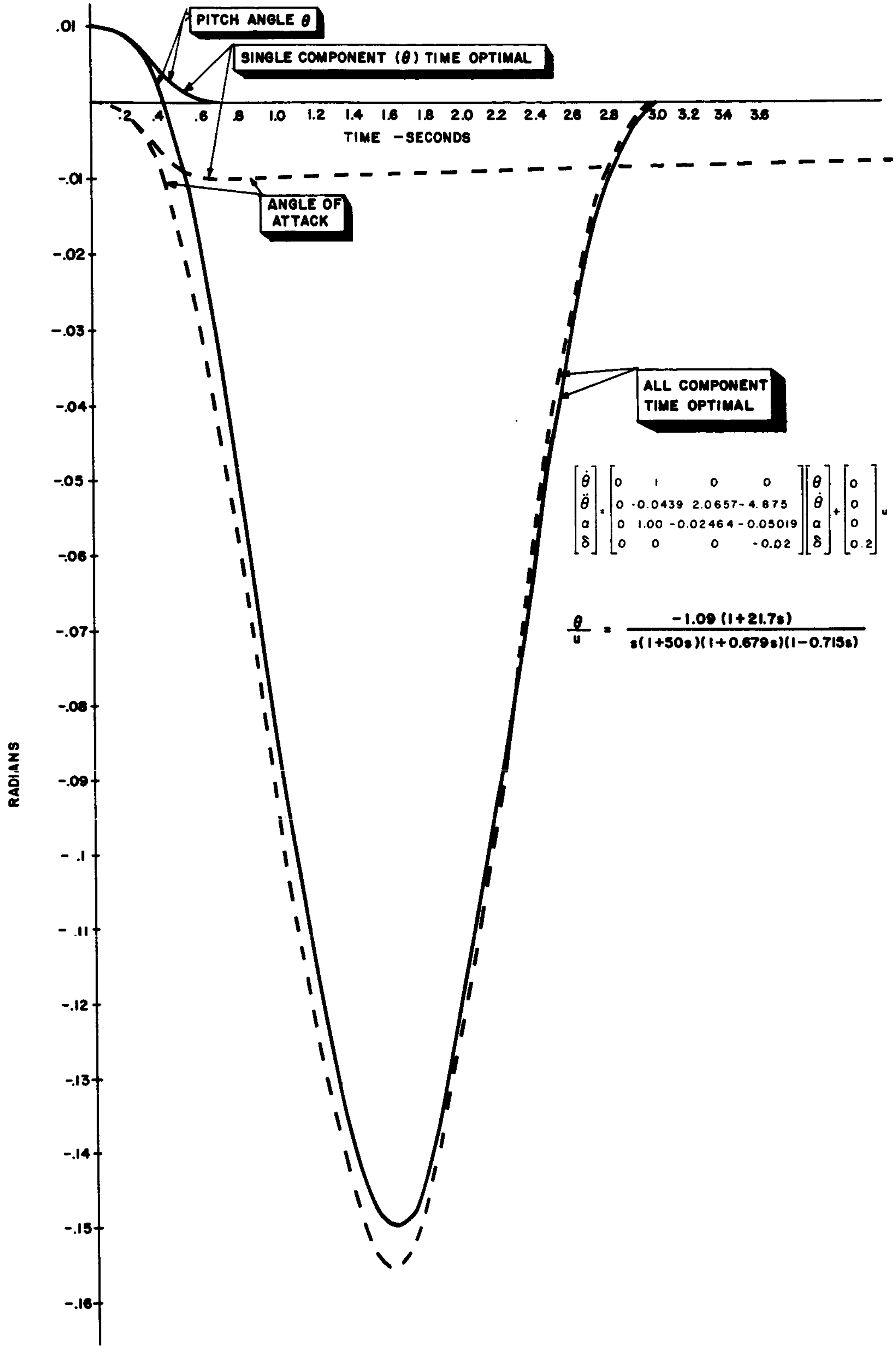

$$\begin{bmatrix}\dot{\theta}\\ \ddot{\theta}\\ \dot{\alpha}\\ \dot{\delta}\end{bmatrix} = \begin{bmatrix}0 & 1 & 0 & 0\\ 0 & -0.0439 & 2.0657 & -4.875\\ 0 & 1.00 & -0.02464 & -0.05019\\ 0 & 0 & 0 & -0.02\end{bmatrix}\begin{bmatrix}\theta\\ \dot{\theta}\\ \alpha\\ \delta\end{bmatrix} + \begin{bmatrix}0\\0\\0\\0.2\end{bmatrix}u$$

$$\frac{\theta}{u} = \frac{-1.09\,(1+21.7s)}{s(1+50s)(1+0.679s)(1-0.715s)}$$

Figure 1. Time Optimal Control of a Rigid Launch Vehicle

[redacted]

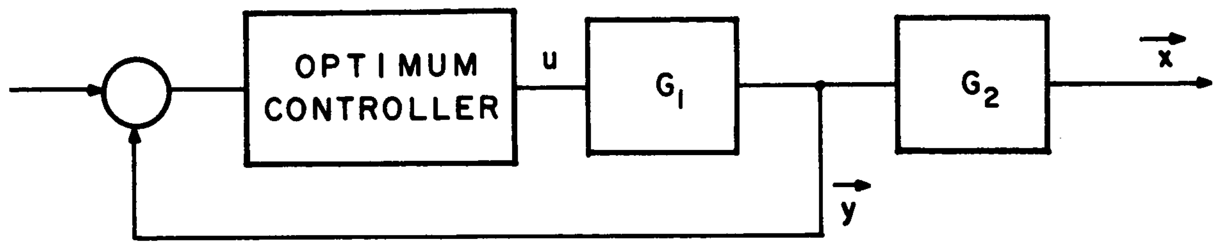

Figure 2. Conceptual Feedback for Controller Synthesis

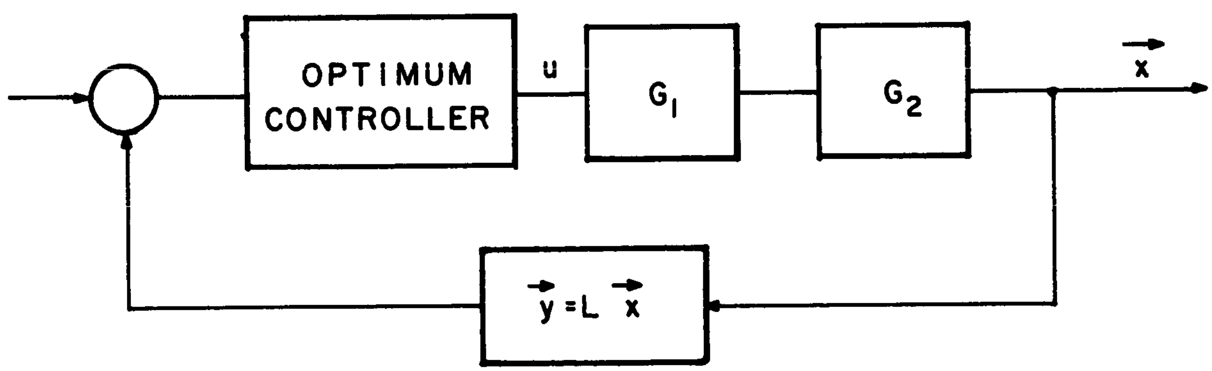

Figure 3. Actual Feedback for Controller Mechanization

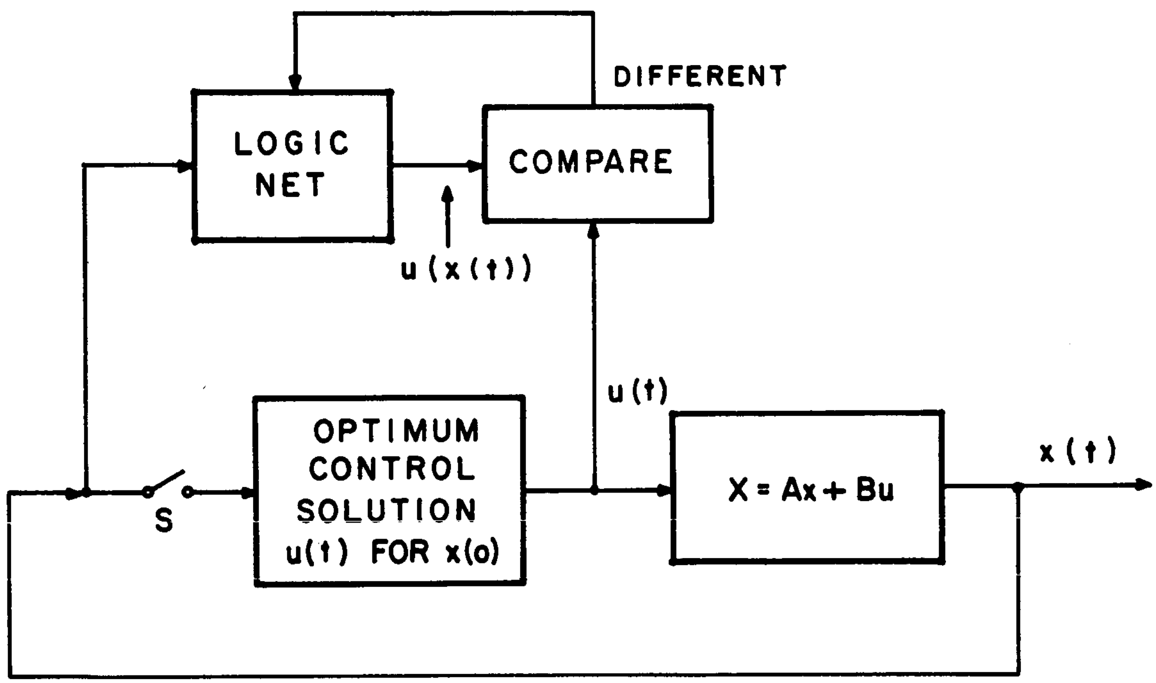

Figure 4. Logic Adjustment Procedure

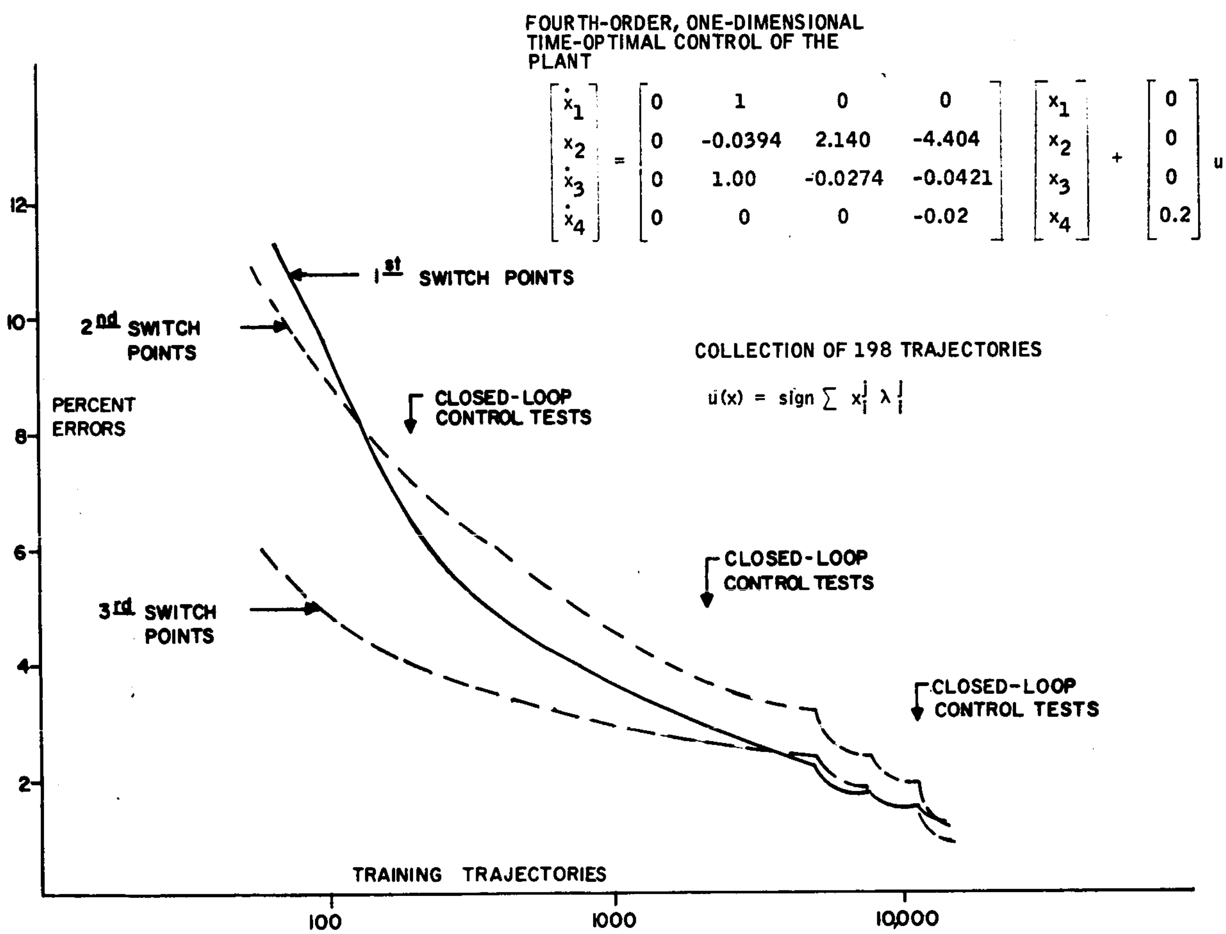

Figure 5. Fourth-order Training Curve

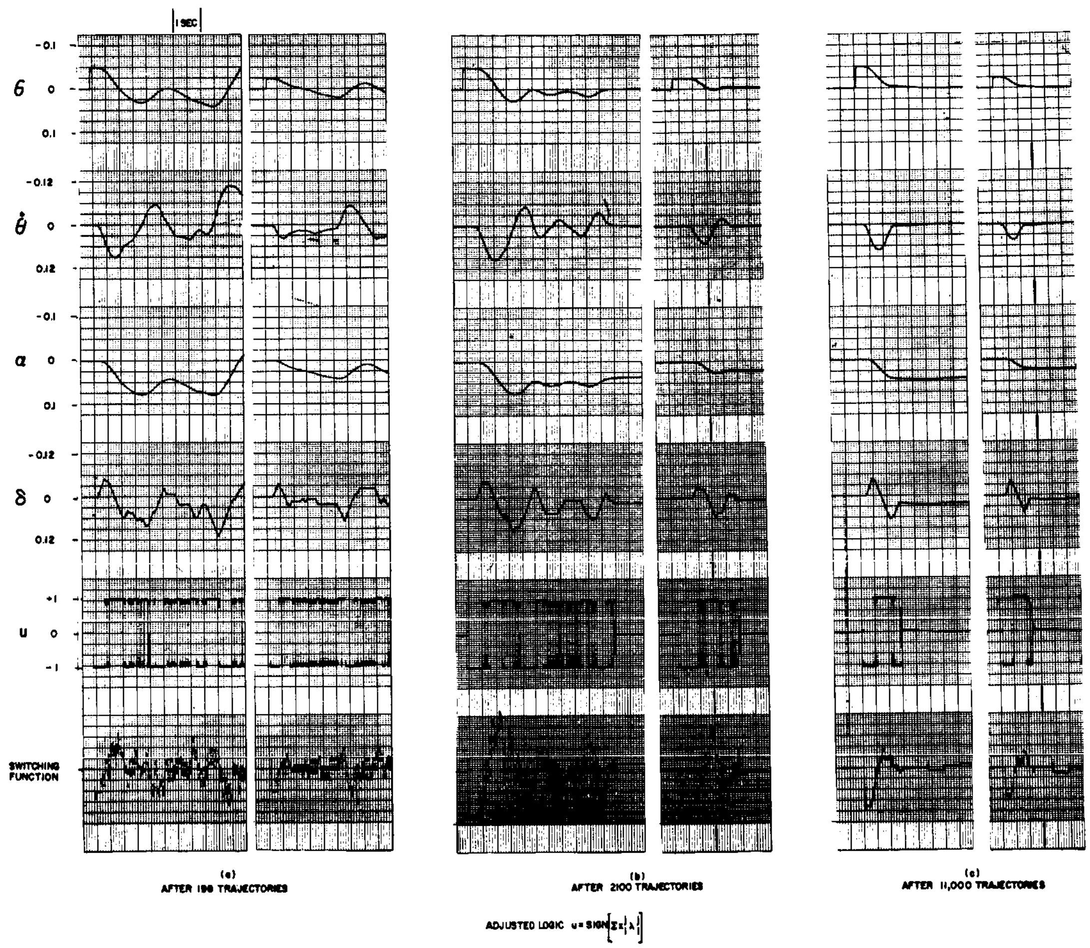

Figure 6. Closed-loop Responses at Three Stages of Training

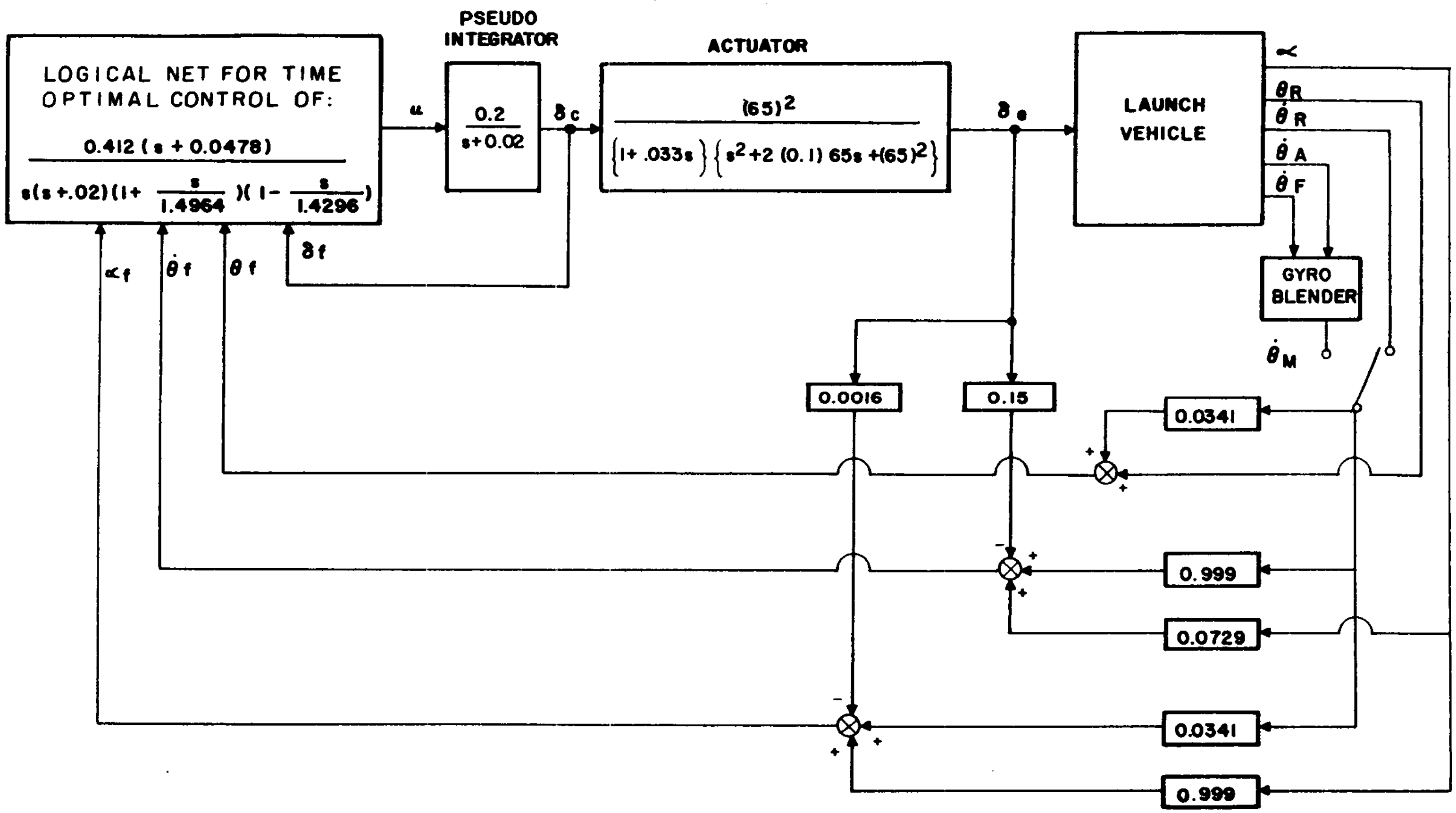

Figure 7. Block Diagram - Fourth-Order Attitude Regulation

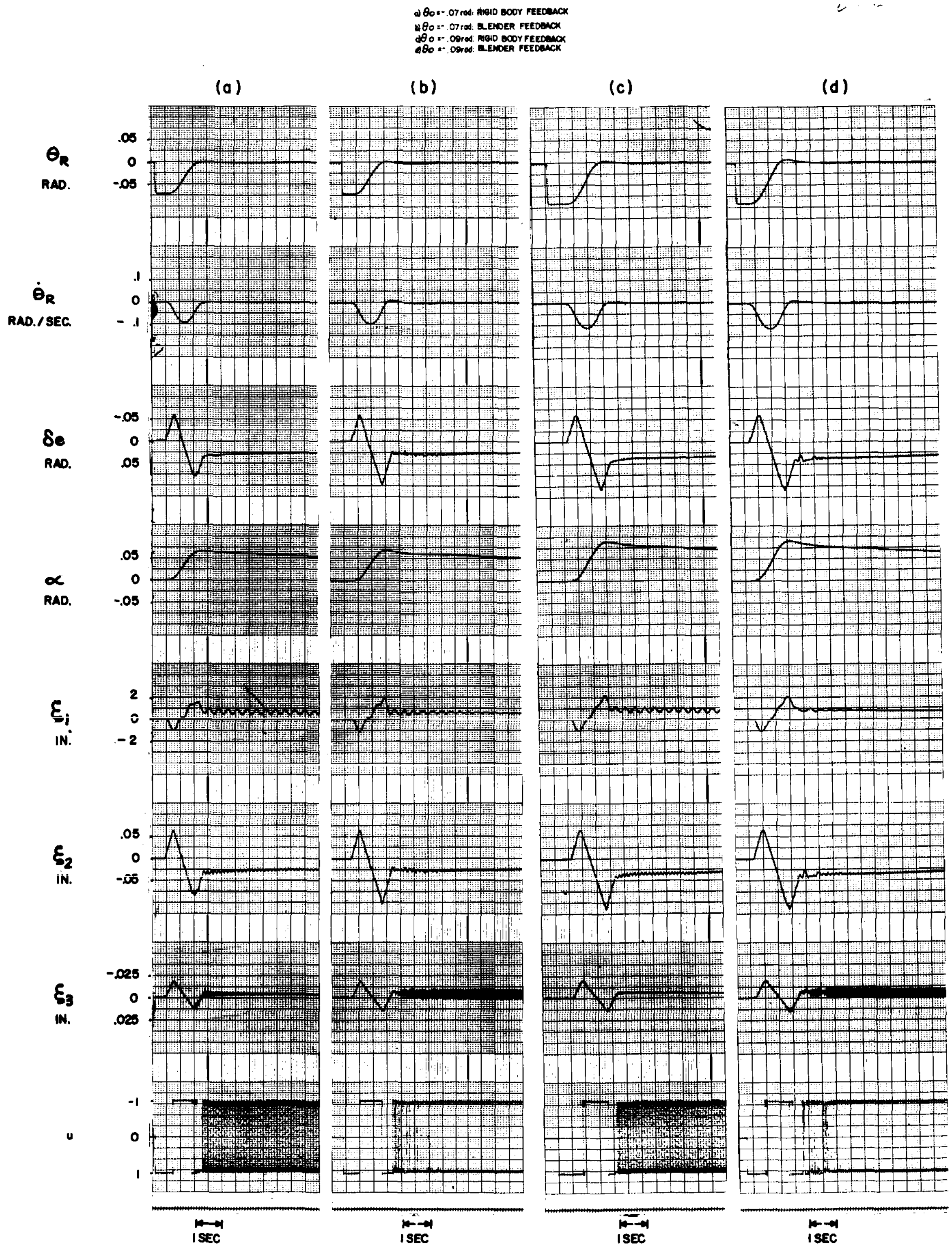

Figure 8. Attitude Regulation - Response to Initial Desplacement Errors

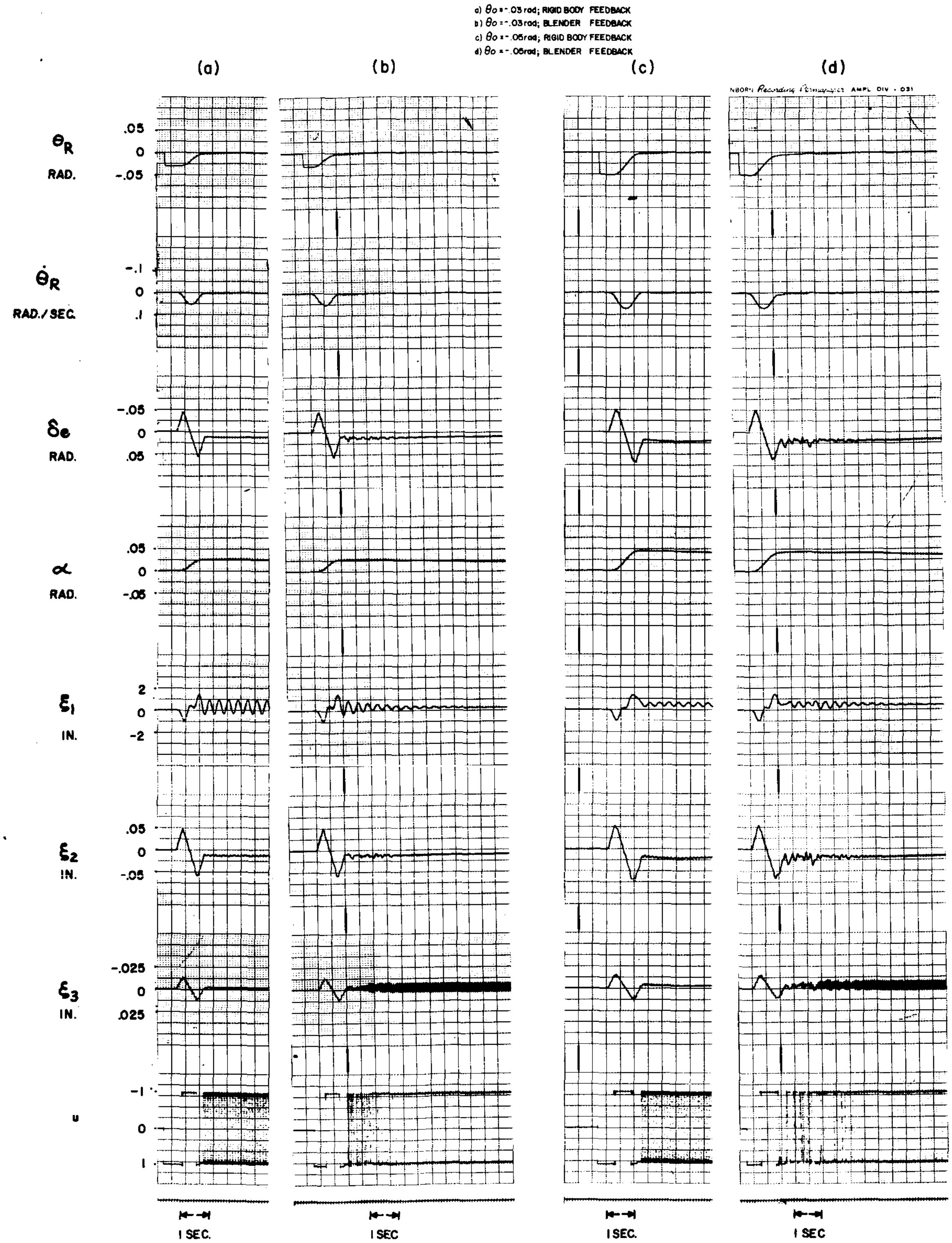

Figure 9. Attitude Regulation - Response to Initial Desplacement Errors

[redacted]

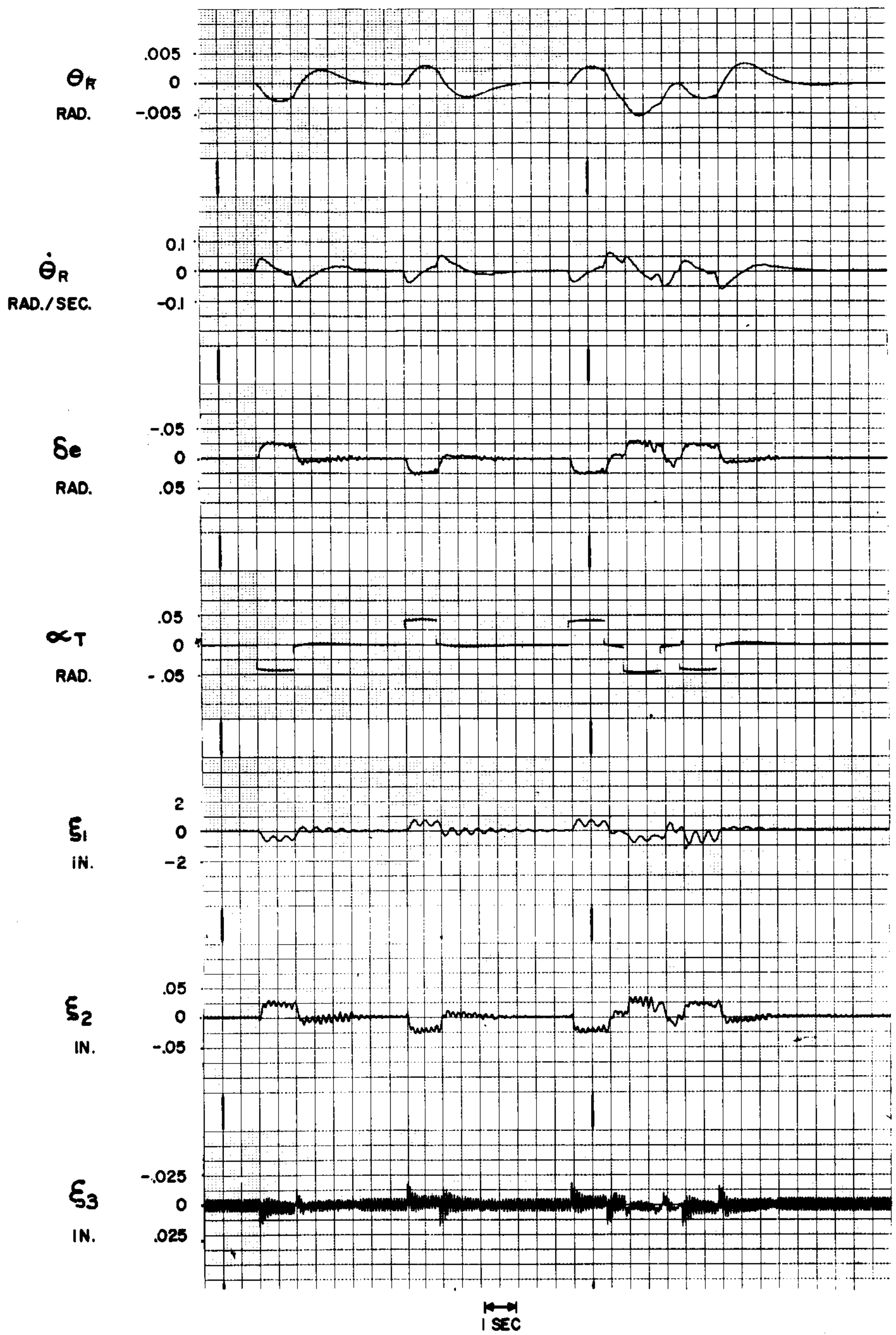

Figure 10. Attitude Regulation - Response to 40 fps Sharp-edge Gust

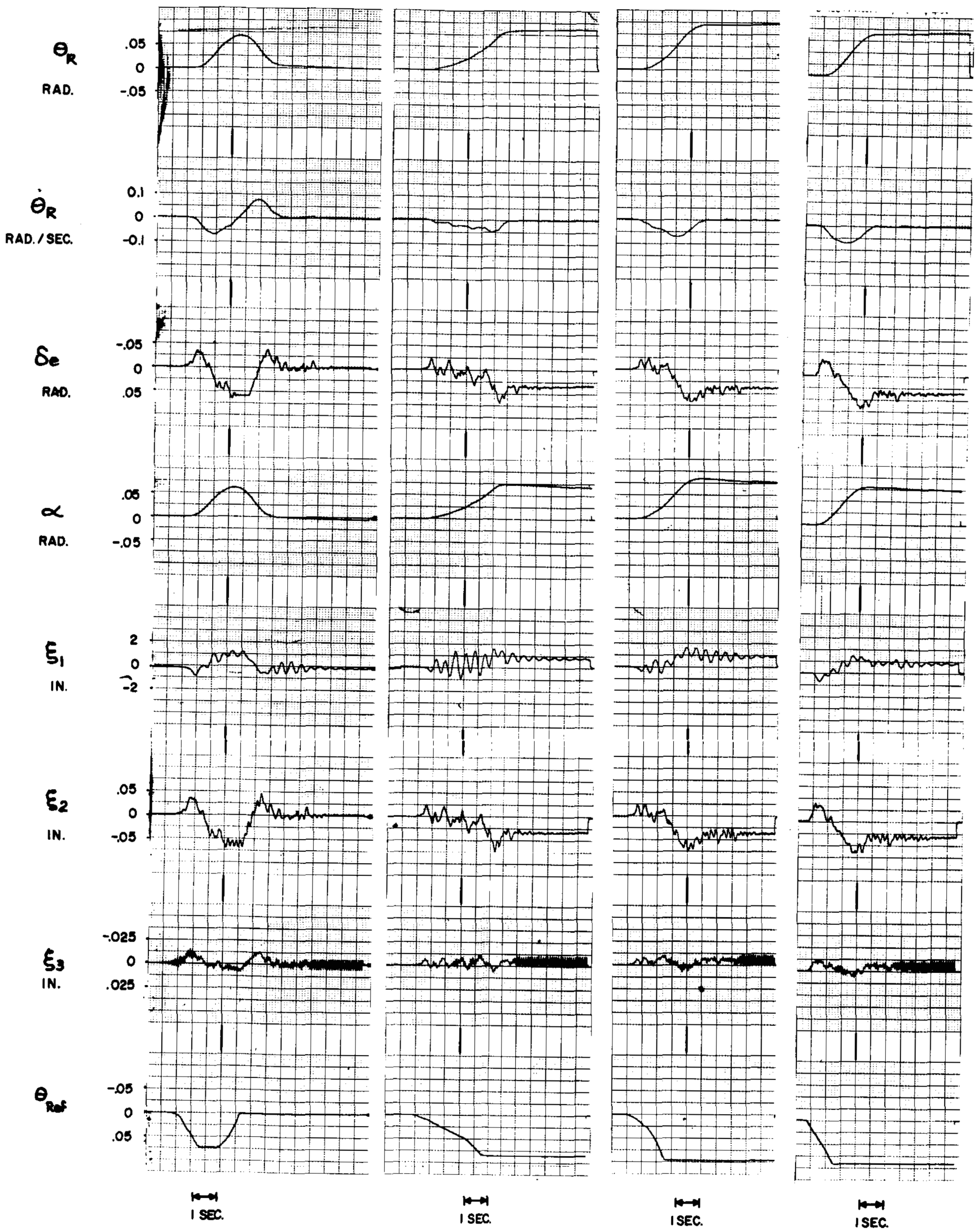

Figure 11. Attitude Control - Response to Command Inputs